Accurate Battery Models Matter: Improving Battery Performance Assessment Using a Novel Energy Management Architecture

Hao Wang^{a,*}, S. Ali Pourmousavi^a, Wen L. Soong^a, Xinan Zhang^b, Rui Yuan^a

^aSchool of Electrical & Mechanical Engineering, The University of Adelaide, Australia ^bSchool of Engineering, The University of Western Australia, Australia

Abstract

Inaccurate modelling of battery energy storage systems (BESSs) leads to significant financial and technical challenges, undermining investment confidence in large-scale BESS projects and other applications and hindering global carbon reduction efforts. This paper underscores the critical need for precise battery modelling using a thorough evaluation of experimental data to illustrate the limitations of inaccurate battery models in remaining energy estimation. In addition, advanced simulation studies are conducted using actual residential data to demonstrate the negative consequences of power mismatch and economic returns using these inaccurate models. Key discoveries highlight how accurate battery models can improve the accuracy of techno-economic evaluation and mitigate investment risks. This is demonstrated using a novel and computationally tractable energy management system (EMS) architecture. Future research should focus on developing standardised modelling protocols and fostering collaboration among manufacturers, researchers, and operators to bridge existing knowledge gaps. By increasing public awareness about the significance of accurate battery modelling and promoting interdisciplinary cooperation, this work aims to drive improved decision-making and accelerate the adoption of reliable, efficient BESS operations in the global transition to sustainable energy systems.

Keywords: Battery modelling, Electrification, Energy storage system, Remaining energy estimation, Techno-economic assessment

Email address: hao.wang05@adelaide.edu.au (Hao Wang)

^{*}Corresponding Author

1. Introduction

The global push toward electrifying various energy demand sectors, driven by concerns over climate change and energy efficiency, underscores the critical role of energy storage in general and electrochemical batteries in particular. Despite significant progress in improving these technologies, batteries remain a costly component in this transition [1, 2]. As demand for electricity grows with electrification, particularly in transportation and industrial sectors, understanding and modelling battery behaviour (e.g., remaining energy of the battery or state of health (SoH)) becomes paramount during planning and operation for economic viability analysis and operational efficiency, which is summarised in Fig. 1 (a).

In transportation, where batteries power increasing numbers of zero-emission vehicles [3], and in industries requiring energy storage to meet fluctuating demand and integrate renewables, the need for batteries is evident. On the other hand, grid-scale batteries, with their rapid response and flexibility [4], are crucial to managing the variability of renewable energy, ensuring grid stability, and facilitating widespread adoption. Various critical applications of batteries are summarised in Fig. 1 (b). However, the economic viability of battery projects can be uncertain because of the high capital cost, replacement costs, and low profit margins, which led to government subsidies to mitigate risks.

In a rapidly electrifying world, where batteries serve as cornerstones in the energy transition, harnessing their full potential is dependent on comprehensive feasibility and techno-economic assessment to guide decision-making and ensure economic and operational success. To that end, accurate battery modelling is crucial not only in project planning but also in operational optimisation. Whether in electric vehicles for range estimation or in stationary applications to prevent overcharging and overdischarging, a precise estimation of the state of charge (SoC), SoH, and dynamic behaviour is indispensable [5, 6]. The importance of adopting extended battery models has recently been identified as a critical challenge in achieving the full value of the system in planning, market, and operational decision-making [7].

In recent years, the limitations of inaccurate BESS models have been identified in research studies and a few computationally efficient battery models have been proposed to improve the remaining energy estimation accuracy for optimal energy dispatch problems with BESS. In [8], the authors proposed a non-ideal linear Li-ion battery model that considers the nonlinear dynamics of the batteries. In their work, the energy mismatch is observed in comparison with other ideal conventional Li-ion battery models. Later, this work was extended in [9] considering the degradation costs of the battery. The simulation results show that the proposed non-ideal model can reduce the error of BESS power mismatch from 13.3% to 3.7%. More related works are presented in [10, 11, 12, 13], where the internal chemical and thermal dynamics of Li-ion batteries are considered to formulate an accurate model for optimal energy dispatch problems. However, considering the complexity of multi-physics modelling for batteries, these solutions can be impractical in real-world operation. In addition, the electrochemical, thermal, and degradation mechanisms of batteries need further detailed modelling to fit simulation studies for long operating cycles. For example, the ohmic overpotential of batteries is often modelled by a constant internal resistance to reduce the nonlinearity of the model. The thermal and electrochemical dynamics of the batteries are often not considered, and the degradation of the batteries is represented by a fitted 1-D curve without considering the actual operation of the battery in the past. These simplifications undermine the accuracy and reliability of these models. Meanwhile, the effect of ambient temperature is not taken into account in the majority of the works. In environments with elevated temperatures, the internal power consumption of the BESS during high-

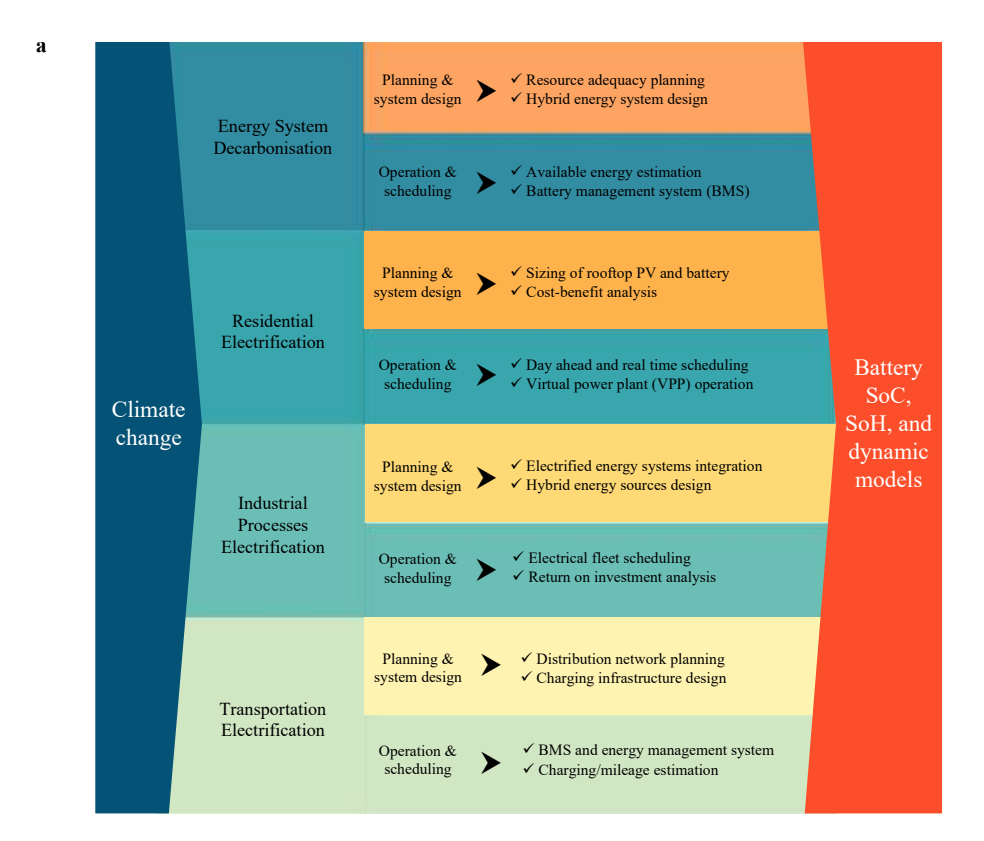




Figure 1: The role of battery energy storage systems (BESSs) in the clean energy transition. (a) The roles of accurate battery models in the planning, design, scheduling and operation stages of different types of electrification projects. (b) Accurate battery modelling brings multiple economic and quality benefits in grid-level or residential-level energy storage projects.

power operation regimes can be more significant, and there is a risk of emergency shutdowns of the BESS or insufficient power output regulated by the battery management system (BMS). These drawbacks result in the low fidelity of these models. Most importantly, there is a lack of compelling validation of the models using real BESS data or widely accepted battery models. Critical battery states, e.g., remaining energy or temperature obtained from simulations or actual BMS, are important to demonstrate the accuracy of these proposed models. For example, during the late period of the charge/discharge process, more dramatic variations in efficiency, as a result of the increase in overpotentials and temperature, lead to a lower estimation accuracy. Inaccurate results in remaining energy estimation and power mismatch could also occur by these models when the BESS operates under extreme ambient temperature and non-intermediate SoC ranges. Most importantly, the inaccurate economic benefits and value assessment of BESS caused by these modelling approaches are not discussed in these works. This could result in significant financial losses due to the unawareness of operators and investors of these issues.

In this paper, we show the limitations of simplified battery models, which could result in significant discrepancies in estimating the remaining energy for four common battery technologies. In addition, we shed light on the impact of limited battery performance information and the use of simplified battery models, which could lead to inaccurate estimation of technical and financial performance, as evidenced in the residential energy arbitrage application in this study. Most importantly, a novel and computationally tractable energy management system (EMS) architecture is proposed to overcome the limitations in simplified battery models by incorporating accurate multi-physics or data-driven battery models.

The rest of the paper is organised as follows: Section 2 explains the definitions of the different remaining energy estimation models and identifies the limitations within these simplified models. Section 3 shows the inaccuracy in remaining energy estimation when using these simplified models, as illustrated by experimental data. Section 4 demonstrates the adverse outcomes resulting from inaccuracies in techno-economic evaluations within optimal energy dispatch scenarios. Lastly, a novel and computationally tractable framework is proposed to improve battery energy dispatch performance and achieve high accuracy.

2. Definitions of remaining energy in batteries

SoC is a universal metric for different types of batteries to indicate the remaining capacity inside a battery. SoC estimation is critical to prevent battery overcharging or over-discharging, and is also used to manage battery power to prevent thermal runaway and mitigate excessive degradation to extend useful life and ensure safe operation [5, 6]. From the battery management perspective, the SoC is the most important indicator for accurate remaining capacity estimation.

To understand the concept of SoC, it is essential to understand the principles of how batteries function. Battery operation relies on the migration of active ions between the anode and the cathode, which facilitates charge and discharge processes that produce a chemical potential essential for extracting or storing electricity. To measure the capacity in a battery considering the mechanism of energy conversion, Faraday's laws of electrolysis are used to describe the relationship between the total charge from the active ions and the electric current. This law indicates that the integration of the total charge change during battery operation can be approximately proportional to the integration of current. In fact, for most commercial battery products, their coulombic efficiency is at a very high level (approximately 99%) [14]. This universal definition of SoC can be mathematically represented neglecting the minor side reaction losses and capacity fading, as follows:

$$SoC_{t} = SoC_{0} + \frac{\int_{0}^{t} I_{c}(t) dt}{C_{n}} - \frac{\int_{0}^{t} I_{d}(t) dt}{C_{n}}$$
 (1)

where the $I_c(t)$ and $I_d(t)$ are the charge and discharge current of the battery at time t, respectively. C_n represents the nominal capacity of the battery in Ah. In numerous studies and tools focused on battery SoC, including those related to battery scheduling in hybrid energy systems or the sizing and design of battery energy storage systems (BESSs), the charge/discharge power profiles are used as the primary input parameters. This is primarily due to the complexity of modelling battery voltage and other operational mechanisms (e.g., charge loss, auxiliary equipment power consumption, etc.). For instance, battery voltage has a nonlinear relationship with the SoC, hence formulating it in an optimisation problem can make it intractable and unsolvable in many cases. As a result, a new definition of energy stored in the battery has evolved over the years, which is referred to as the state of energy (SoE), and is mathematically defined in [15], as given below:

$$SoE_t = SoE_0 - \frac{\int_0^t P_d(t) dt}{E_n}$$
 (2)

where $P_d(t)$ is the discharge power at time t and E_n is the nominal energy in kWh or Wh. The SoE formulation here is used to estimate the remaining energy during discharge. To extend its application to the charging processes, another universal definition considers the charge power $P_c(t)$ at time t as follows:

$$SoE_{t} = SoE_{0} - \frac{\int_{0}^{t} P_{d}(t) dt}{E_{n}} + \eta_{r} \frac{\int_{0}^{t} P_{c}(t) dt}{E_{n}}$$
(3)

The definition in Eq. (3) uses the same nominal energy as Eq. (2) with a constant round-trip efficiency η_r . These values can be conveniently found or derived using the information on the battery datasheet. However, relying on the nominal energy and constant round-trip efficiency could potentially lead to significant errors in estimating the remaining energy inside a BESS. In practice, the remaining energy estimation results using Eq. (3) potentially yield significant discrepancies compared with accurate estimation results using SoC measurement by the BMS. The reason is that these values are normally measured for a specific operational condition (e.g., constant power/current regime, normal room temperature environment), namely ideal conditions. As such, any changes in the battery operation (e.g., partial charge and discharge) and thermal dynamics of the BESSs will consequently cause substantial variations in their available energy and efficiency. In this case, the BESS is operated under a non-ideal condition in which the ambient temperature and operational power may perform significantly differently from the specified operational condition. In [7], the authors emphasise that achieving an accurate estimate of the remaining energy in a BESS is crucial to realise their full value. Inaccurate estimation can severely influence the operation of BESSs in many aspects that will cause financial losses, financial mismatch (inaccurate BESS economic benefits/revenue estimation) and unsatisfied consumers and investors.

3. Investigation of remaining energy estimation error in the mainstream BESS technologies

To show the remaining energy estimation discrepancies using SoC and SoE definitions under different operational conditions, we selected four distinct battery technologies, three Li-ion bat-

teries, namely A123 Systems ANR26650m1-B, Panasonic NCR-18650B, LG Chem INR21700-M50, and a 5 kW/3 kWh (rated) vanadium redox flow battery (VRFB) system, shown in Table 1, for which extensive data was available online or through our collaborators [16]. In particular, the experimental data for the three Li-ion batteries are obtained from Stanford Energy Control Laboratory [17], and the data for the VRFB system is obtained from our collaborators [16]. The experiments are carried out under different galvanostatic discharge currents while maintaining an ambient temperature at 25°C. Fig. 2 shows the SoE and SoC results obtained based on the nominal capacity values in Ah and the nominal energy values in Wh based on the information given in the datasheets using Eq. (2) and Eq. (1) respectively, which are shown in Table 1.

Table 1: The specifications of the four batteries in this study [16, 18, 19, 20]

	Panasonic NCR-18650B (NCA)	LG Chem INR21700-M50 (NMC)	A123 Systems ANR26650m1-B (LFP)	VRFB
Nominal capacity C_n (Ah)	3.35	5	2.5	60
Nominal voltage (V)	3.6	3.63	3.3	50
Nominal energy E_n (Wh)	12.1	18.2	8.3	3000

The results of the four galvanostatic discharge tests indicate that the disparity between SoE and SoC becomes more apparent as the operational time and discharge current increase. This discrepancy is attributed to variations in operational conditions that influence the losses incurred within the battery. Alternatively, variations in battery operation efficiency contribute to inaccuracy in estimating the remaining energy using a simplistic SoE method from Eq. (2). As a result, the efficacy of this simple SoE model in precisely estimating the remaining energy is contingent on the operational environment closely resembling the specific testing conditions under which these typical performance metrics were obtained. For instance, when faced with different operational conditions, as evidenced in the case of the LFP, NCA, and NMC batteries, and the VRFB in Figs. 2 (a-d), where their nominal energy is evaluated using these typical performance metrics or under ideal discharge conditions (normally low current discharge or neglect the voltage variations), simple SoE models cannot accurately estimate the remaining energy. This demonstrates the non-ideal outcomes in estimating the remaining energy that we have postulated. Moreover, from all the error bars in the last column of Figs. 2 (a-d), we can observe that the discrepancies tend to increase as the operational conditions become more non-ideal.

Note that the Li-ion batteries chosen for our study are single-cell devices, allowing applied discharge currents to exceed 3C. However, in most medium- or large-scale BESSs, the allowable maximum discharge current managed by the BMS is generally not greater than 2C. For these BESSs, we expect to see a discrepancy caused by variations in the efficiency of the charging and discharging process and discharge energy due to the change in battery power and degradation level, the power consumption of the auxiliary equipment (for thermal management, power management, etc.), self-discharge losses, variations in environmental temperature, and other potential factors with impact on round-trip efficiency. Overlooking these factors in the remaining energy estimation methods can result in technical issues and financial mismatches in the optimal BESS dispatch problem. The next section investigates this impact in detail.

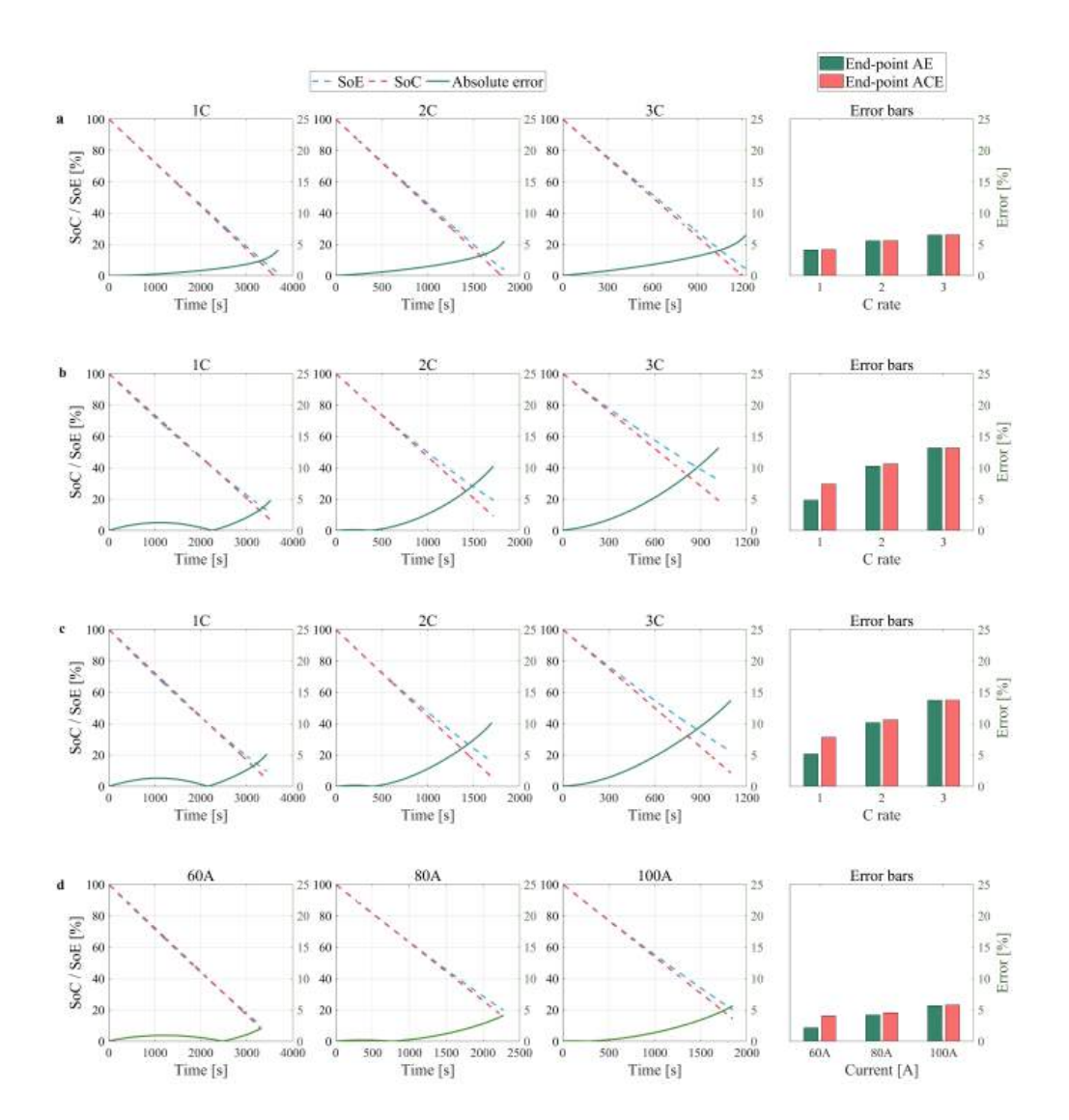


Figure 2: The SoC and SoE profiles of four BESS technologies. Three Li-ion batteries (LFP, NCA, NMC) are tested in 25°C controlled chamber under galvanostatic discharge currents of 1C, 2C and 3C until they reached the cut-off voltage limits [17]. Also, a 5 kW/3 kWh (rated) VRFB system was tested at 25°C room temperature under galvanostatic discharge currents of 60 A, 80 A, and 100 A until the cut-off voltage limit was reached. The SoC and SoE are derived using Eq. (1) and Eq. (2), and two error metrics, namely absolute error (AE) and absolute cumulative error (ACE), are adopted to quantify the discrepancy between SoE and SoC values. The end-point ACE and AE in the last column are the values at the last timestep of each discharging process. Each row shows the SoE, SoC and error profile results obtained for one of the batteries in the mix: (a) A123 Systems ANR26650m1-B. (b) Panasonic NCR-18650B. (c) LG Chem INR21700-M50. (d) 5 kW/3 kWh VRFB system.

4. Energy estimation and optimal BESS operation: A case study

Non-ideal operation of BESS often leads to notable fluctuations in efficiency, primarily driven by variations in charge/discharge power necessary to meet system-level operational demands. This observation is supported by the outcomes of our analysis shown in Fig. 2 (d) for a VRFB. However, it is crucial to quantify the magnitude of this impact at the system level, e.g., inaccurate remaining energy estimation inside the BESS and inaccurate BESS economic benefits estimation outcomes (financial mismatch) incurred during battery asset operation. Considering data availability and operational complexity, we decided to run our simulation study for 40 residential cases with rooftop PVs and batteries from the Australian Capital Territory (ACT), Australia using the NextGen dataset [21]. These 40 residential cases are randomly selected from a large part with 20 cases in July 2022 and 20 cases in February 2023. These cases have a range of load demands and PV solar generation profiles requiring different battery operations during typical summer and winter periods. We used one-day load demand and PV generation profiles for our analysis. We assumed that all the users in these cases own a 5 kW/10 kWh VRFB system on their premises, and perfect load demand and PV generation prediction are available to reduce the complexity of the study and keep our focus on the financial outcome related to battery energy estimation. We assumed that each household owns a home energy management system (HEMS) that operates the battery and rooftop PVs to minimise the electricity cost (in Appendix C). The round-trip efficiency of this 5 kW/10 kWh VRFB system in the SoE model is assumed to be 70% based on the ideal charge/discharge tests (in Appendix B), which are used in the decision-making processes of the HEMS. The simulation results are shown in Figs. 3 (a-e) for one of the users. Figs. 3 (a-b) shows the load and PV generation profiles, the time of use (ToU) tariff and the solar feed-in tariff (FiT). In this setup, the HEMS solves an optimisation problem for 24 hours ahead at 5-minute interval, and the commands are transmitted to the battery BMS to follow. We ran another simulation study using the command from HEMS based on a multi-physics model (in Appendix A) to simulate the actual battery operation. Accurate SoC estimation results are adopted for each of the cases as the real-time remaining capacity estimation trajectory. The estimated remaining energy in SoE is obtained from the HEMS by Eq. (3) before the BESS operation.

It can be observed from Fig. 3 (c) that the remaining energy of the BESS estimated by the HEMS is considerably different from the actual SoC with a peak absolute error of about 8%. The actual round-trip efficiency is 66.1% versus the ideal efficiency of 70% due to the standby power consumption of the BESSs, side reactions, and overpotential losses. As a consequence, the discrepancy between the estimated and actual measurement increases with the operation time, as can be seen in Fig. 4 (a) for 40 cases. Furthermore, the actual and scheduled BESS power mismatch is shown in Fig. 3 (d) for a single user, where the BESS optimal power has not been fully realised. Finally, the financial impact of the power mismatch, as a result of the error in the remaining energy estimate, is shown in Fig. 4 (b) for all cases. It can be seen that the HEMS overestimated the economic benefits when using a constant round-trip efficiency obtained from ideal test conditions. This critical issue also tends to occur in other BESS technologies such as Li-ion batteries during actual operation. As a result, there is an inevitable mismatch between the actual economic benefits of BESSs and the estimated benefits by HEMS, which can be quite significant from the simulation results. Furthermore, in [23], Lin et al. presented a comprehensive study that reveals multiple critical factors influencing the efficiency of Li-ion batteries, mainly temperature, current, voltage, and capacity degradation. A previous work by Noyanbayev et al. in [24] analysed a grid-connected BESS, and found that the round-trip efficiency of the Li-ion BESS could have a maximum difference of around 6% in different constant power

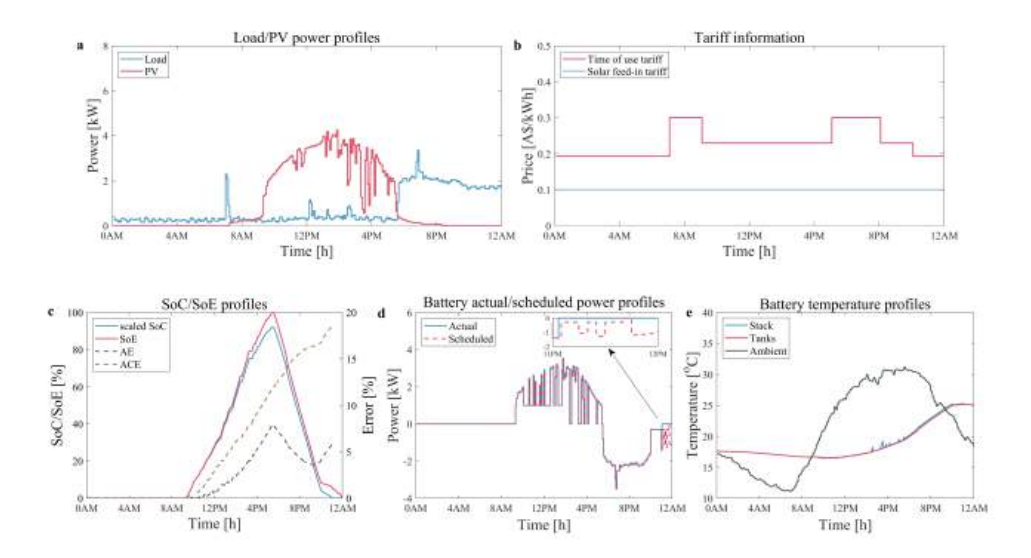
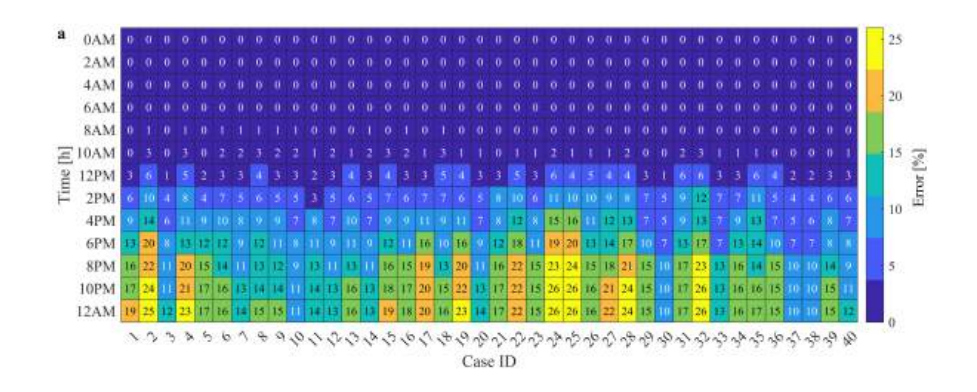


Figure 3: The simulation results obtained for a 5 kW/10 kWh VRFB system from an optimal BESS energy dispatch problem for a single unidentified residential user in ACT, Australia on February 16th, 2023 as an example. In this simulation study, a time of use (ToU) electricity tariff and a solar feed-in tariff (FiT) from Origin Energy in ACT, Australia are adopted [22]. The actual PV generation and load profiles are obtained for this residential user. The SoC and SoE mismatch and their impact on operation cost are calculated. Perfect forecast data is assumed here to focus the simulation studies and analysis on the impact of SoE inaccuracy. The SoC values are scaled based on the upper and lower allowable system SoC limits (10-95%) managed by the BMS, to 0-100% to indicate the available remaining capacity. In this figure, we see: (a) the load and PV generation profiles of the anonymous user, (b) the ToU tariff and solar FiT data, (c) the estimated SoE, real-time SoC profiles and the absolute error (AE) and absolute cumulative error (ACE) between the estimated SoE and the real-time SoC in daily operation, (d) the BESS power schedule and the actual power of the BESS, and (e) the ambient temperature and VRFB temperature profiles.

charge/discharge operational regimes (60-240 kW) from 0%-100%-0% SoC range. These studies illustrate that using a constant value for efficiency is not sufficient to accurately measure the actual performance of a Li-ion BESS under various conditions. Moreover, considering usable energy and degradation of BESSs under different charging and discharging conditions is necessary to ensure accurate remaining energy estimation and techno-economic evaluation outcomes. In Fig. 5, we summarise the potential factors that contribute to the inaccurate remaining energy estimation and the results of the techno-economic evaluation at different stages and outline the potential consequences, which can result in unsatisfied customers and investors.

BESS industry stakeholders have made significant contributions to the advancement of energy storage technologies, and addressing the above challenges is essential for customers and users to evaluate the performance and economic value of BESS precisely. These issues appear to be solvable considering the actual efficiency of BESSs. Upon closer examination, three main concerns emerge: (1) limited information availability to fully analyse the actual performance of BESS under different operational conditions, (2) lack of comprehensive experimental data for accurate model formulation, and (3) insufficient knowledge or tendency to over-simplify battery models among stakeholders. In Table 2, we list information on six popular commercial BESS products from their product datasheets. Although generic information related to the efficiency or usable energy available in battery datasheets can provide a preliminary understanding of the BESS, operators and designers can benefit from more practical information to form a comprehen-



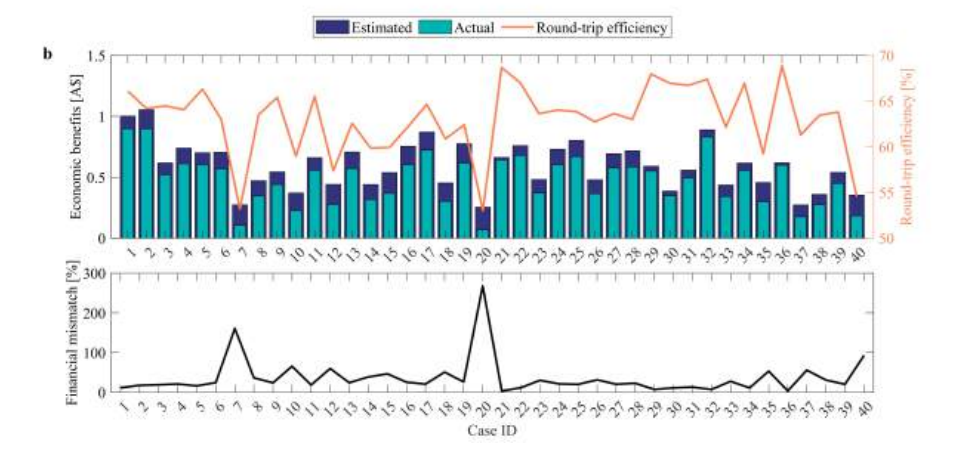


Figure 4: The simulation results for 40 unidentified residential cases from an optimal BESS energy dispatch problem in ACT during July 2022 and February 2023. The SoC and SoE mismatch and their impact on operation cost are calculated. The processes and assumptions are identical to the single unidentified residential case analysis as noted in the caption of Fig. 3. (a) the percentage ACE between the estimated SoE and the real-time SoC for all cases, and (b) the estimated and actual economic benefits of the VRFB system for the 40 residential cases, and the actual round-trip efficiency of the VRFB system for a day along with the absolute percentage error (APE) between the estimated and actual economic benefits for all cases.

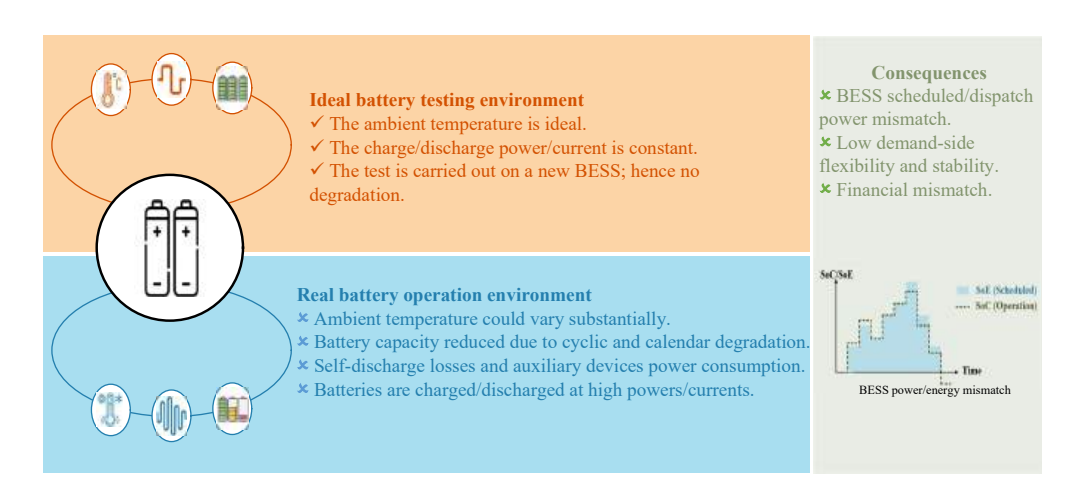


Figure 5: The underlying factors that cause the performance discrepancy between the ideal and real operational environments and the consequences.

Table 2: Examples of the BESS performance metrics from the product datasheet

No.	Type	Test conditions	Efficiency & Usable energy	Ref.
1	Li-ion	3.3 kW charge & discharge power at 25°C	90% (AC), 13.5 kWh	[25]
2	Li-ion	100% depth of discharge (DOD), 0.2C charge & discharge at 25°C	Not available, 6.4–25.6 kWh	[26]
3	Li-ion	100% DOD, 0.2C charge & discharge at 25° C	≥95%, 5 kWh (DC)	[27]
4	Li-ion	95% DOD at 25°C	Not available, 9.3 kWh	[28]
5	Li-ion	Not available	Not available, 7.8 kWh for each module	[29]
6	VRFB	5.6 kW, 7.2 kW, 10 kW, 12 kW, 14 kW charge & discharge power	76–84%, 28–45 kWh (efficiency & discharge energy under different power regimes) 77% nominal efficiency (DC, with pump losses) 72% nominal efficiency (AC) 40 kWh rated energy	[30]

sive understanding of the actual performance of the system, which is essential for precise BESS sizing, effective planning, and optimal operation scheduling. For example, the usable energy and actual efficiency of BESSs are essential performance indicators, which may vary depending on operational scenarios and ambient temperature conditions. In addition, factors such as capacity deterioration and other forms of degradation are crucial mechanisms that must be considered. Furthermore, the limited experimental analysis of BESS systems is another critical factor that restricts the development of accurate battery models to improve BESS operation. Additional information is required from experimental or field operational data analysis of these BESSs to estimate the performance metrics of the BESS products under actual operation. We also see a general lack of understanding of SoC and SoE in the academic literature. Consequently, in almost every related work in the literature, the definitions of SoC and SoE are confused with

the common practice of referring to SoE as SoC. Moreover, the variations in the efficiency of batteries are generally not considered, and the definition of remaining energy in the BESS is relatively vague. In addition, these simplified models for energy management studies neglect many operational mechanisms within BESSs which are important for precisely simulating their actual dynamics, as introduced in Section 1.

We regard the proposition of simplified numerical models as generally challenging and impractical for accurately estimating the remaining energy in BESSs. It will require continuous monitoring of voltaic efficiency and coulombic efficiency, which can be performed by non-linear observers and machine learning methods during battery operation [31]. However, these sophisticated models require substantial computational resources to solve optimal energy dispatch problems; hence, they become computationally impractical in real-world applications. Additionally, constructing precise numerical models necessitates an in-depth understanding of the BESS operational mechanisms, which originates from detailed knowledge of battery chemistry. Also, high-quality BESS operational data and reliable experimental analysis are required to do this. These factors potentially result in a lack of reliable and computationally efficient modelling approaches to tackle the problem of imprecise residual energy estimation in BESS over a long period considering all the operational dynamics.

5. Introducing an iterative approach for optimisation-based applications as a potential solution

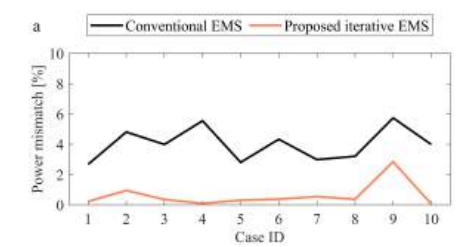
Many battery applications introduced in Fig. 1 require an optimisation problem to be solved, which means that incorporating the instantaneous voltage efficiency of BESS is impractical. Therefore, the real question is how we can integrate highly accurate BESS models into the BESS planning or operation optimisation problem to improve the accuracy of decisions. Here, we propose a novel yet computationally tractable EMS architecture, presented in Fig. 6 (b), as opposed to the traditional EMS shown in Fig. 6 (a), which integrates the EMS with an accurate and computationally efficient BESS model. This iterative EMS combines highly accurate BESS models to provide an accurate round-trip efficiency to the decision-making process in the optimisation problem. The proposed solution is evaluated using 40 randomly selected residential cases as indicated in the previous section. We anticipate that the proposed EMS will result in a reduced discrepancy between the scheduled and actual battery power, as well as a more accurate economic estimate compared to traditional EMS. The simulation results are presented in Figs. 6 (c-d), where the proposed method significantly improved the accuracy of the estimation of BESS dispatchable energy as well as the estimated economic benefit to customers. The mean power mismatch errors have decreased from 5.2% to 0.5%, whereas the mean financial mismatch errors have reduced from 36.8% to 2.3%.

Another critical issue for BESS technologies is degradation, which results in the decay of usable capacity, usable energy, and efficiency. The degradation mechanisms of BESS introduce various levels of uncertainty in modelling, which could potentially lead to increased discrepancies in both power and financial mismatch results for BESS. To rigorously validate the proposed EMS architecture, we considered a realistic scenario for this 5 kW/10 kWh VRFB system with an electrolyte volume imbalance of 80 L between the two tanks during operation. This not only results in degradation of the capacity of the VRFB system but also causes a change in the crossover rate due to the more rapid variations in the vanadium ion concentration driven by diffusion. In this case, the nominal energy capacity of the BESS is 8.8 kWh using the identical procedures presented in Appendix B. To showcase the robustness of the proposed iterative EMS architecture



Figure 6: The proposed iterative EMS approach and performance evaluation of 40 different cases in February and July (perfect forecast data is assumed). (a) Schematic diagram of a conventional EMS without considering the operational dynamics of the BESS. (b) Schematic diagram of the proposed iterative EMS that incorporates the actual round-trip efficiency of the BESS. (c) The absolute percentage error (APE) between the scheduled and actual BESS power over a day by two different EMS approaches (typical EMS in the literature and the proposed solution in this paper) of the 40 residential cases. (d) The APE between the estimated economic benefit and the actual economic benefit of the two different EMS approaches for the 40 residential cases.

and to account for the real-world performance of a BMS that struggles to precisely measure the remaining energy during BESS operation, the nominal energy for testing is assumed to be 8.5 kWh and remains constant throughout the operation of the iterative EMS. This value is estimated



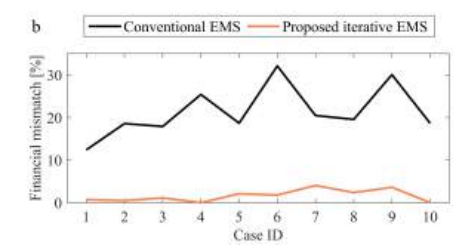


Figure 7: The performance evaluation of the iterative EMS method incorporating a highly accurate BESS model with degradation to overcome increased uncertainties in conventional remaining energy estimation. The APE between (a) the scheduled and actual BESS power and (b) the estimated economic benefit and the actual economic benefit, over a day by two different EMSs for the 10 residential cases in February.

using a straightforward estimator based on a modification of Faraday's law of electrolysis as:

$$E'_{n} = E_{n} \cdot \frac{\min(V_{half}^{n}, V_{half}^{p})}{V_{half}}$$

$$\tag{4}$$

Here, $E_n^{'}$ is the nominal energy after degradation. V_{half}^n , V_{half}^p and V_{half} are the half-system volumes on the negative and positive half-system after the electrolyte transferal, and the electrolyte volume in the tanks without electrolyte transfer, respectively. The initial round-trip efficiency used in the proposed EMS architecture is 70%, and E'_n is used to determine the optimal BESS dispatch energy schedule until it satisfies the stop criteria shown in Fig. 6 (b). The performance of the proposed iterative EMS architecture considering degradation for the 10 cases is shown in Fig. 7. Note that in this new case study, we select 10 profiles in February 2023 which have sufficient solar generation compared with the data in July 2022 so that the capacity of the BESS can be better utilised (achieving a higher depth of discharge (DOD) range around or higher than 60%). In this case, the impact of battery degradation, capacity, and other factors on the actual working performance of the BESS can be more significant, allowing for a thorough evaluation of the proposed EMS. The simulation results obtained from the new case study also demonstrate the effectiveness of the proposed iterative EMS in reducing power mismatch errors and financial errors (mean power mismatch error reduced from 4.0% to 0.6%, mean financial mismatch error reduced from 21.4% to 1.6%). More importantly, the proposed method does not increase the computational complexity of the optimisation problem while guaranteeing high accuracy in estimating the efficiency of the BESS system. Most of the instances were solved in only two iterations, whereas the maximum number of iterations was only three. The average computational time for each cycle is less than 10 seconds on an Intel(R) Core(TM) i7-10700 CPU of 2.90 GHz with 16 GB of RAM, which can be further improved using more computationally efficient BESS models (e.g., machine learning models). An alternative approach to handling computational demands, if needed, is to host the optimisation problem within a cloud solution. This setup allows the local HEMS to simply communicate with the cloud and obtain the optimisation results for implementation.

To facilitate a better understanding of the strengths and challenges associated with popular battery modelling types and their potential use within the proposed EMS framework, we have gathered common battery models from literature in Table 3. This table outlines the strengths, shortcomings, and feasibility of integrating them into the suggested iterative EMS framework to

refine the techno-economic evaluation of BESS. Equivalent circuit models (ECMs) and mixed-integer formulations are the most commonly used models in EMS-related literature, as mentioned earlier, which generally lack the accuracy to facilitate EMS operation in determining the optimal energy dispatch schedule. These simple models greatly impede the accuracy of the remaining energy estimation, leading to numerous adverse effects detailed in Section 4.

Table 3: Mainstream battery modelling approaches and their strengths, shortcomings, and the practicality of incorporating them in the proposed iterative EMS framework

Types	Pros	Cons Co	mpatibility
Multi-physics	Generic and easy to adopt for identical battery type. Good battery state observability and interpretability.	Requires additional consideration of BMS operation. Low robustness due to parameter variations. Could be computationally intensive (High-dimensional finite element models).	/
Data-driven	Universal for different battery types. Computationally efficient to use after training. High accuracy without prior knowledge of BMS and battery.	Low interpretability. Extensive computational resources are required for training. Performance depends on the quality of training.	✓ data.
Equivalent circuit	Good accuracy with adaptive observers to tackle parameter variations. Available to integrate with other electric systems. Computationally efficient for real-time control and state estimation.	Low accuracy without accurate real-time senso for battery parameter identification. Extensive analysis of high-quality experimental data is required for model formulation.	rs X
Mixed-integer formulation	Designed to be used in optimal BESS energy dispatch schedule or optimal sizing problems.	Extensive computational resources are needed to find the optimal solution with nonlinear formulation. Linear formulation may significantly lack accuracy.	х

Despite the notable improvements achieved by the proposed EMS framework, there is still a mismatch between the EMS schedules and actual battery operation. This is mainly due to the lack of precise tracking of instantaneous voltage efficiency at each optimisation interval that prevents the achievement of a near-zero estimation error of the remaining energy in real-time operation. Addressing this complex issue requires additional research efforts via experimental analysis and close cooperation with battery manufacturers and operators of BESS. However, the effort required can differ greatly depending on the type of battery technology. For example, LFP batteries, recognised for their stable voltage efficiency, yield fairly precise results even when a constant round-trip efficiency is used in conventional SoE estimation techniques [17]. However, for other Li-ion battery chemistries, such as NCA and NMC, which are characterised by poorer thermal performance and higher internal resistance, additional considerations are imperative for modelling nonlinear variations in voltage and temperature. Similarly, VRFBs, distinguished by their high thermal stability but nonlinear overpotential characteristics, benefit from nonlinear equations for overpotential modelling because of the stability of their voltage behaviour. These diverse battery characteristics can assist operators in developing efficient and highly accurate MILP (mixed-integer linear programming) models. This contributes to optimising BESS operation and conducting more precise techno-economic assessments during the planning phase, thereby substantially augmenting the revenue of BESS projects, reducing financial risks for investors, and helping policymakers make better decisions. Another issue is that the majority of data-driven models for batteries in the existing literature are only capable of real-time simulation or estimation of a single battery's state (e.g., SoC, SoH, etc.) while other system states (e.g., voltage, current, temperature, etc.), may not be available but are required by the proposed iterative EMS framework which requires accurate and predictive multi-output estimations. This emphasises the necessity of developing multi-output models that can accurately simulate BESS operation based on scheduled operational inputs (e.g., temperature, power load profiles, initial SoC, etc.). These models should be capable of precisely predicting multiple output parameters over the optimisation time horizon (e.g. SoC, voltage, active species concentration, etc.). Nowadays, physics-informed machine learning approaches have gained significant traction, which can ensure the accuracy of multi-output predictions with limited numbers of inputs by incorporating universal electrochemical, chemical, and mechanical laws with limited input data during training.

6. Conclusions

Inaccurate estimation of the remaining energy in BESSs can result in unattainable energy dispatch outcomes, leading to less than optimal economic returns that could threaten end-user satisfaction and increase the risk of investment in battery projects. While the impact of this problem may differ across various battery technologies, most current battery technologies can be significantly affected. In this paper, the limitations of simple battery models are quantified through the experimental analysis of Li-ion batteries and VRFBs in inaccurate remaining energy estimation. Subsequently, the detrimental effects of these imprecise battery models on energy dispatch and economic returns are illustrated through a residential energy arbitrage application. Given the essential role of BESSs in the decarbonisation of transportation, heavy industries such as mining, and the electric grid, this may have severe financial consequences and potentially hinder decarbonisation initiatives among various electrification sectors. Therefore, this study aims primarily to raise awareness among BESS operators and investors to refine existing practices. We also have developed and evaluated a practical solution that can be applied in numerous studies focused on BESS planning and operation.

Analysing comprehensive experimental battery data aids in enhancing the performance of current battery models; hence, interdisciplinary collaboration among researchers with diverse expertise in electrochemistry, mechanical engineering, electrical engineering, and energy is essential. Furthermore, testing the performance of the proposed EMS framework using actual BESSs and developing accurate MILP battery models that consider all the operational mechanisms are promising areas of future work to bring additional benefits to BESS users.

Acknowledgment

This project is supported by the Australian Government Research Training Program (RTP) through the University of Adelaide, and a supplementary scholarship is provided by the Microgrid Battery Deployment project, which is funded by the Future Battery Industries Cooperative Research Centre (FBICRC) as part of the Commonwealth Cooperative Research Centre Program, Australia.

Appendix A. Multi-physics vanadium redox flow battery thermal model

The proposed model is developed to simulate the vanadium species variations in the tanks and stacks under the mass balance law, where the thermal modelling part is established and follows

the energy balance law based on the work by Tang et al. in [32] and extended by Wang et al. using an industrial-scale VRFB system with the 5 kW stack configuration reported in [33, 34, 35].

For vanadium ions in the stack:

$$\frac{V_s}{2} \frac{dc_2^s}{dt} = Q_s \left(c_2^t - c_2^s \right) \pm \frac{NI}{zF} - Nk_2 \frac{c_2^s}{D} S - 2Nk_5 \frac{c_5^s}{D} S - Nk_4 \frac{c_4^s}{D} S$$
 (5)

$$\frac{V_s}{2} \frac{dc_3^s}{dt} = Q_s \left(c_3^t - c_3^s \right) \mp \frac{NI}{zF} - Nk_3 \frac{c_3^s}{D} S + 3Nk_5 \frac{c_5^s}{D} S + 2Nk_4 \frac{c_4^s}{D} S$$
 (6)

$$\frac{V_s}{2} \frac{dc_4^s}{dt} = Q_s \left(c_4^t - c_4^s \right) \mp \frac{NI}{zF} - Nk_4 \frac{c_4^s}{D} S + 3Nk_2 \frac{c_2^s}{D} S + 2Nk_3 \frac{c_3^s}{D} S$$
 (7)

$$\frac{V_s}{2} \frac{dc_5^s}{dt} = Q_s \left(c_5^t - c_5^s \right) \pm \frac{NI}{zF} - Nk_5 \frac{c_5^s}{D} S - 2Nk_2 \frac{c_2^s}{D} S - Nk_3 \frac{c_3^s}{D} S$$
 (8)

For vanadium ions in the tanks:

$$V_n \frac{dc_2^t}{dt} = Q_s \left(c_2^s - c_2^t \right) \tag{9}$$

$$V_n \frac{dc_3^t}{dt} = Q_s \left(c_3^s - c_3^t \right) \tag{10}$$

$$V_p \frac{dc_4^t}{dt} = Q_s \left(c_4^s - c_4^t \right) \tag{11}$$

$$V_{p}\frac{dc_{5}^{t}}{dt} = Q_{s}\left(c_{5}^{s} - c_{5}^{t}\right) \tag{12}$$

$$E^{OCV} = E^{0'} + \frac{RT}{zF} \ln \left(\frac{c_2^s c_5^s}{c_3^s c_4^s} \right)$$
 (13)

The overall stack voltage during charging is

$$E_{s} = N \left[E^{0'} + \frac{RT}{zF} \ln \left(\frac{c_{2}^{s} c_{5}^{s}}{c_{3}^{s} c_{4}^{s}} \right) + ir' - \frac{RT}{zF} \ln \left(1 - \frac{I}{k_{m} F L_{e} H_{e} c_{3}^{s}} \right) - \frac{RT}{zF} \ln \left(1 - \frac{I}{k_{m} F L_{e} H_{e} c_{4}^{s}} \right) \right]$$
(14)

The stack voltage during discharging is:

$$E_{s} = N \left[E^{0'} + \frac{RT}{zF} \ln \left(\frac{c_{2}^{s} c_{5}^{s}}{c_{5}^{s} c_{4}^{s}} \right) - ir' + \frac{RT}{zF} \ln \left(1 - \frac{I}{k_{m} F L_{e} H_{e} c_{5}^{s}} \right) + \frac{RT}{zF} \ln \left(1 - \frac{I}{k_{m} F L_{e} H_{e} c_{5}^{s}} \right) \right]$$
(15)

$$k_m = 1.6 \times 10^{-3} \left(\frac{Q_c}{10 L_e W_e} \right)^{0.4} \tag{16}$$

Note k_m is the mass transfer coefficient in dm s⁻¹, and in this form the units for Q_c , L_e and W_e are L s⁻¹, dm and dm, correspondingly [34]. The electrolyte temperature in the stack:

$$C_p \rho V_s \frac{dT_s}{dt} = Q_s C_p \rho \left(T_p - T_s \right) + Q_s C_p \rho \left(T_n - T_s \right) + I^2 R_s + I T_s \frac{dE}{dT} + P_{self}$$

$$\tag{17}$$

The electrolyte temperature in the positive/negative tanks are:

$$C_p \rho V_p \frac{dT_p}{dt} = Q_s C_p \rho \left(T_s - T_p \right) + U_t A_t \left(T_{air} - T_p \right)$$
(18)

$$C_{p}\rho V_{n}\frac{dT_{n}}{dt} = Q_{s}C_{p}\rho \left(T_{s}-T_{n}\right) + U_{t}A_{t}\left(T_{air}-T_{n}\right) \tag{19}$$
 The definition and value of variables and definitions are given in Table 4 below:

Table 4: Model parameters and their definitions

	System states	
Symbol	Definition	Unit
c_i^s, c_i^t	Concentration of i-th vanadium ion in stack and tank	mol L ⁻¹
E_s	Stack voltage	V
T_s, T_p, T_n	Electrolyte temperature in stack, positive and negative tank	°C
T_{air}	Outside air temperature	°C
I	Applied current	A
i	Applied current density	A m ⁻²
P_{self}	Self-discharge losses (detailed derivation can be found in [35])	W
	Parameters	
Symbol	Definition	Value
N	Number of cells in the stack	37
V_p, V_n	Volume of the electrolyte in the positive/negative tank	240 L
V_s	Volume of the electrolyte in the stack	40 L
H_e, L_e, W_e	Height, length and width of the electrode	$0.3, 0.7, 2.5 \times 10^{-3} \text{m}$
S	Membrane area	0.21 m^2
D	Thickness of the membrane	$1.27 \times 10^{-4} \text{ m}$
R	Gas constant	$8.314 \text{ J mol}^{-1} \text{ K}^{-1}$
Q_s, Q_c	System flow rate and cell flow rate	$0.278,0.0075\;\mathrm{L\;s^{-1}}$
ρ	Electrolyte density	1.3kg dm^{-3}
ρ F	Faraday's constant	96,485 C mol ⁻¹
r'	Overall cell resistivity	$2.72~\Omega~\text{cm}^2$
R_s	Overall stack resistance	$0.048~\Omega$
k_2	Diffusion coefficient of V ²⁺	$8.768 \times 10^{-12} \text{ m}^2\text{s}^{-1}$
k_3	Diffusion coefficient of V ³⁺	$3.222 \times 10^{-12} \text{ m}^2 \text{s}^{-1}$
k_4	Diffusion coefficient of V ⁴⁺	$6.825 \times 10^{-12} \text{ m}^2\text{s}^{-1}$
k ₅	Diffusion coefficient of V ⁵⁺	$5.897 \times 10^{-12} \text{ m}^2 \text{s}^{-1}$
$E^{0'}$	Formal potential	1.40 V
A_t	Surface area of the tank	2.8 m^2
U_t	Overall heat transfer capability of the tank	$3.67 \text{ J K}^{-1} \text{ s}^{-1} \text{ m}^{-2}$
ρ	Electrolyte density	1.354 g cm ⁻³
C_p	Specific heat capacity of electrolyte	$3.2 \mathrm{J}\mathrm{g}^{-1}\mathrm{K}^{-1}$

Appendix B. Capacity and efficiency of the 5 kW/10 kWh VRFB system

The actual capacity and system efficiency of the proposed $5 \, kW/10 \, kWh \, VRFB$ system in the energy management study is obtained from the simulation results using constant current (CC)-constant voltage (CV)/constant power (CP)-CV for charging and CC/CP for discharge based on the definition in [36].

Table 5: Performance of the proposed 5 kW/10 kWh VRFB system under different simulation studies

Current/ Power	SoC range	DOD	η_{rt}	Discharge energy
100 A	28.7-92.6%	63.9%	68.28%	7.97 kWh
80 A	22.8-92.5%	69.7%	69.97%	8.79 kWh
60 A	17.1-92.8%	75.7%	70.72%	9.50 kWh
40 A	11.3-92.9%	81.6%	67.60%	9.99 kWh (Nominal energy)
20 A	10.0-92.9%	82.9%	54.66%	9.02 kWh
5000 W	36.7-92.7%	56.0%	68.06%	7.01 kWh
4000 W	28.5-92.5%	64.0%	69.70%	8.09 kWh
3000 W	21.0-92.5%	71.5%	70.29%	9.02 kWh
2000 W	14.0-92.8%	78.7%	67.96%	9.69 kWh
1000 W	10.0-92.9%	82.9%	55.40%	9.14 kWh

$$\eta_s = \frac{\int_{t_0}^{t_f} (P_d - P_{aux}) dt}{\int_{t_0}^{t_f} (P_c + P_{aux}) dt}$$
 (20)

$$E_{dch} = \int_{t_0}^{t_f} (P_d - P_{aux}) dt$$
 (21)

Here, P_c , P_d and P_{aux} are the battery charge power, battery discharge power, and battery auxiliary power.

Appendix C. Home energy management system (HEMS)

Objective (minimise electricity cost):

$$\min \sum_{t \in \mathcal{H}} \left(C_t^{im} P_t^{im} \right) \Delta t - \left(C_t^{ex} P_t^{ex} \right) \Delta t \tag{22}$$

Battery operational constraint:

$$SoE_{t} = SoE_{t-1} + \eta_{r} \frac{P_{t}^{ch} u_{t}^{ch} \Delta t}{E_{n}} - \frac{(P_{t}^{dch} - P^{aux}) u_{t}^{dch} \Delta t}{E_{n}}, \quad \forall t \in \mathcal{H}$$
 (23)

$$SoE_{min} \le SoE_t \le SoE_{max}, \quad \forall t \in \mathcal{H}$$
 (24)

$$0 \le u_t^{ch} + u_t^{dch} \le 1, \quad \forall t \in \mathcal{H}$$
 (25)

$$P_{min}^{ch} + P^{aux} \le P_t^{ch} \le \min\left(\alpha_{ch} + \beta_{ch} P_{max}^{ch}, P_{max}^{ch}\right) + P^{aux}, \quad \forall t \in \mathcal{H}$$
 (26)

$$P_{min}^{dch} + P^{aux} \le P_t^{dch} \le \min\left(\alpha_{dch} + \beta_{dch}P_{max}^{dch}, P_{max}^{dch}\right) + P^{aux}, \quad \forall t \in \mathcal{H}$$
 (27)

When
$$t = t_0 \& t_f$$
 $SoE_t = 0$, $\forall t \in \mathcal{H}$ (28)

Load power balance:

$$P_t^{pv} + (P_t^{dch} - P^{aux}) \cdot u_t^{dch} \cdot \eta_{inv} - P_t^{ch} \cdot u_t^{ch} / \eta_{inv} = P_t^{ex} - P_t^{im} + P_t^{load}, \quad \forall t \in \mathcal{H}$$
 (29)

Table 6: The definition of symbols, their value and type in the HEMS formulation for optimal energy dispatch of the 5~kW/10~kWh~VRFB system (The DV in the table stands for decision variable and the coefficients for battery charging/discharging power regulation are designed to fully charge or discharge the VRFB system)

Symbol	Definition	Туре
C_t^{im}	Cost of imported electricity at timestep t (Time of use tariff in A\$/kWh)	Variable
C_t^{ex}	Revenue of exported electricity to the grid at timestep t (Solar feed-in tariff in A\$/kWh)	Variable
P_t^{im}	Residential imported power from the grid at timestep t in kW	Real number DV
P_t^{ex}	Residential exported power to the grid at timestep t in kW	Real number DV
SOE_t	Estimated remaining energy in the battery at timestep t in %	Variable
u_t^{ch}	Battery status indicator during charging at timestep <i>t</i> (1: in charging, 0: idle)	Binary DV
u_{\star}^{dch}	Battery status indicator during discharging at timestep t (1: in discharging, 0: idle)	Binary DV
P_t^{ch}	Battery charge power at timestep t in kW	Real number DV
P_t^{ch} P_t^{dch} P_t^{pv} P_t^{load}	Battery discharge power at timestep t in kW	Real number DV
P_t^{pv}	PV power generation at timestep t in kW	Variable
P_t^{load}	Load power at timestep t in kW	Variable
P_{min}^{ch}	Minimum charge power (1 kW)	Constant
P_{min}^{dch}	Minimum discharge power (0.2 kW)	Constant
P_{max}^{ch}	Maximum charge power (5 kW)	Constant
P_{dch}^{max}	Maximum discharge power (5 kW)	Constant
Paux	Auxiliary power of the VRFB (0.1 kW)	Constant
α^{ch}	Coefficient in Eq. (26) for battery charging power regulation (10 kW)	Constant
β^{ch}	Coefficient in Eq. (26) for battery charging power regulation (-9 kW)	Constant
α^{dch}	Coefficient in Eq. (27) for battery discharging power regulation (1 kW)	Constant
β^{dch}	Coefficient in Eq. (27) for battery discharging power regulation (6 kW)	Constant
E_n	Nominal (rated) energy capacity of the VRFB system (10 kWh)	Constant
SOE_{min}	Minimum SOE level during the operation (0)	Constant
SOE_{max}	Maximum SOE level during the operation (100%)	Constant
η_{inv}	DC-AC Inverter/AC-DC battery charger efficiency (95%)	Constant
η_{rt}	Round-trip efficiency of the 5 kW/10 kWh VRFB system (70%)	Constant

References

- [1] H. Ritchie, The price of batteries has declined by 97% in the last three decades, Our World in Datahttps://ourworldindata.org/battery-price-decline (2021).
- [2] K. Mongird, V. V. Viswanathan, P. J. Balducci, M. J. E. Alam, V. Fotedar, V. S. Koritarov, B. Hadjerioua, Energy storage technology and cost characterization report, Tech. rep., Pacific Northwest National Lab (PNNL), Richland, WA, United States, https://energystorage.pnnl.gov/pdf/PNNL-28866.pdf (2019).
- [3] E. James, S. Shazan, I. Chingis, O. Conor, Fuel cell electric vehicles 2024-2044: Markets, technologies, and forecasts, https://www.idtechex.com/en/research-report/fuel-cell-electric-vehicles-2024-2044-markets-technologies-and-forecasts/977 (December 2023)
- [4] Australian Renewable Energy Agency, Battery storage, https://arena.gov.au/renewable-energy/battery-storage/(March 2024).
- [5] X. Lin, K. Khosravinia, X. Hu, J. Li, W. Lu, Lithium plating mechanism, detection, and mitigation in lithium-ion batteries, Progress in Energy and Combustion Science 87 (2021) 100953.
- [6] P. V. Chombo, Y. Laoonual, A review of safety strategies of a Li-ion battery, Journal of Power Sources 478 (2020) 228649.
- [7] T. Levin, J. Bistline, R. Sioshansi, W. J. Cole, J. Kwon, S. P. Burger, G. W. Crabtree, J. D. Jenkins, R. O'Neil, M. Korpås, et al., Energy storage solutions to decarbonize electricity through enhanced capacity expansion modelling, Nature Energy (2023) 1–10.
- [8] A. J. Gonzalez-Castellanos, D. Pozo, A. Bischi, Non-ideal linear operation model for Li-ion batteries, IEEE Transactions on Power Systems 35 (1) (2019) 672–682.
- [9] K. Antoniadou-Plytaria, D. Steen, O. Carlson, M. A. F. Ghazvini, et al., Market-based energy management model of a building microgrid considering battery degradation, IEEE Transactions on Smart Grid 12 (2) (2020) 1794–1804.
- [10] Y. Chen, K. Zheng, Y. Gu, J. Wang, Q. Chen, Optimal energy dispatch of grid-connected electric vehicle considering lithium battery electrochemical model, IEEE Transactions on Smart Grid 15 (3) (2023) 3000–3015.
- [11] H. Pandžić, V. Bobanac, An accurate charging model of battery energy storage, IEEE Transactions on Power Systems 34 (2) (2018) 1416–1426.
- [12] J. Tan, X. Chen, Y. Bu, F. Wang, J. Wang, X. Huang, Z. Hu, L. Liu, C. Lin, C. Meng, et al., Incorporating FFTA based safety assessment of lithium-ion battery energy storage systems in multi-objective optimization for integrated energy systems, Applied Energy 367 (2024) 123472.
- [13] H. Shin, R. Baldick, Optimal battery energy storage control for multi-service provision using a semidefinite programming-based battery model, IEEE Transactions on Sustainable Energy 14 (4) (2023) 2192–2204.
- [14] Y. Zheng, M. Ouyang, L. Lu, J. Li, Z. Zhang, X. Li, Study on the correlation between state of charge and coulombic efficiency for commercial lithium ion batteries, Journal of Power Sources 289 (2015) 81–90.
- [15] X. Hu, F. Feng, K. Liu, L. Zhang, J. Xie, B. Liu, State estimation for advanced battery management: Key challenges and future trends, Renewable and Sustainable Energy Reviews 114 (2019) 109334.
- [16] B. Xiong, J. Tang, Y. Li, C. Xie, Z. Wang, X. Zhang, H. B. Gooi, Design of a two-stage control strategy of vanadium redox flow battery energy storage systems for grid application, IEEE Transactions on Sustainable Energy 13 (4) (2022) 2079–2091.
- [17] E. Catenaro, S. Onori, Experimental data of lithium-ion batteries under galvanostatic discharge tests at different rates and temperatures of operation, Data in Brief 35 (2021) 106894.
- [18] LG Chem, PRODUCT SPECIFICATION Rechargeable Lithium Ion Battery Model: INR21700 M50 18.20Wh, https://www.dnkpower.com/wp-content/uploads/2019/02/LG-INR21700-M50-Datasheet.pdf (Accessed:10th March 2024).
- [19] A123 systems, A123 Systems ANR26650M1-B datasheet, https://www.batteryspace.com/prod-specs/6610.pdf (Accessed:10th March 2024).
- [20] Panasonic, Panasonic NCR 18650B datasheet, https://www.imrbatteries.com/content/panasonic_ncr18650b-2.pdf (Accessed:10th March 2024).
- [21] M. Shaw, B. Sturmberg, L. Guo, X. Gao, E. Ratnam, L. Blackhall, The nextgen energy storage trial in the ACT, Australia, in: Proceedings of the Tenth ACM International Conference on Future Energy Systems, 2019, pp. 439–442.
- [22] Origin Energy, Electricity and natural gas offers, https://www.originenergy.com.au/(December 2023).
- [23] Z. Lin, D. Li, Y. Zou, Energy efficiency of lithium-ion batteries: Influential factors and long-term degradation, Journal of Energy Storage 74 (2023) 109386.
- [24] N. Noyanbayev, A. Forsyth, T. Feehally, Efficiency analysis for a grid-connected battery energy storage system, Materials Today: Proceedings 5 (11) (2018) 22811–22818.
- [25] Tesla, Tesla Powerwall 2 Datasheet Australia and New Zealand, https://www.tesla.com/sites/default/files/pdfs/powerwall/Powerwall%202_AC_Datasheet_en_AU.pdf (Accessed:13th December 2024).

- [26] Sungrow, Sungrow-hv-battery-datasheet-sbr064-256.pdf, https://solarjuice.com.au/wp-content/uploads/2023/11/Sungrow-HV-battery-Datasheet-SBR064-256.pdf (Accessed:13th December 2024).
- [27] BYD, Byd-battery-box-lv-flex-datasheet, https://www.bydbatterybox.com/uploads/downloads/BYD_Battery-Box_LV_Flex_Datasheet_V1.4-62b3f4c515a23.pdf (Accessed:13th December 2024).
- [28] LG, Resul0h-r-datasheet-verl.0-170221, https://www.lghomebattery.com.au/_files/ugd/5684f3_ 38c5abe5acdc4343ad31c7a157e781d8.pdf (Accessed:13th December 2024).
- [29] Alphaess, Datasheet-EN-SMILE-T10-HV-V04.13092022, https://www.alphaess.com/Public/Uploads/uploadfile/files/20221122/Datasheet_EN_SMILE-T10-HV_V04.13092022.pdf (Accessed:13th December 2024).
- [30] Rongke Power, Upower datasheet, http://www.rongkepower.com/upload/about/upowerchanpinguigeshushineiban3429.pdf (Accessed:13th December 2024).
- [31] H. He, Y. Zhang, R. Xiong, C. Wang, A novel gaussian model based battery state estimation approach: State-of-energy, Applied Energy 151 (2015) 41–48.
- [32] A. Tang, J. Bao, M. Skyllas-Kazacos, Thermal modelling of battery configuration and self-discharge reactions in vanadium redox flow battery, Journal of Power Sources 216 (2012) 489–501.
- [33] H. Wang, S. A. Pourmousavi, W. L. Soong, X. Zhang, N. Ertugrul, B. Xiong, Model-based nonlinear dynamic optimisation for the optimal flow rate of vanadium redox flow batteries, Journal of Energy Storage 68 (2023) 107741.
- [34] H. Wang, S. A. Pourmousavi, Y. Li, W. L. Soong, X. Zhang, B. Xiong, A new zero-dimensional dynamic model to study the capacity loss mechanism of vanadium redox flow batteries, Journal of Power Sources 603 (2024) 234428.
- [35] H. Wang, W. L. Soong, S. A. Pourmousavi, X. Zhang, N. Ertugrul, B. Xiong, Thermal dynamics assessment of vanadium redox flow batteries and thermal management by active temperature control, Journal of Power Sources 570 (2023) 233027.
- [36] A. Tang, J. Bao, M. Skyllas-Kazacos, Studies on pressure losses and flow rate optimization in vanadium redox flow battery, Journal of power sources 248 (2014) 154–162.